Entanglement generation through an open quantum dot: Exact two-electron scattering state in the Anderson model

Takashi Imamura,* Akinori Nishino,† and Naomichi Hatano‡
Institute of Industrial Science, The University of Tokyo, 4-6-1 Komaba, Meguro-ku, Tokyo 153-8505, Japan
(Received 19 November 2009; published 29 December 2009)

We analytically study entanglement generation through an open quantum-dot system described by the two-lead Anderson model. We exactly obtain the transition rate between the nonentangled incident state in one lead and the outgoing spin-singlet state in the other lead. We find that only the spin-singlet state can transmit in the cotunneling process. To discuss such an entanglement property in the open quantum system, we construct the exact two-electron scattering state of the Anderson model. It is striking that the scattering state contains spin-singlet bound states induced by the Coulomb interaction. The bound state describes a scattering process in which the set of momenta is not conserved and hence, it is not in the form of a Bethe eigenstate.

DOI: 10.1103/PhysRevB.80.245323 PACS number(s): 03.67.Bg, 03.65.Nk, 05.60.Gg, 73.63.Kv

I. INTRODUCTION

We present an exact approach to electron entanglement generation in an open quantum system. Entanglement has attracted much attention in wide range of physics; it is a resource for quantum information processing and provides insight into quantum phase transitions in statistical physics.[1,2] In most studies, the entanglement properties are discussed in closed systems in equilibrium. In order to study manipulation of entanglement, however, we need to consider an open system out of equilibrium. Entanglement generation using electrons in mesoscopic structures has been proposed recently.[3–8] In Refs. 3, 4, and 8, in particular, devices are connected to reservoirs, electrons enter the device from the reservoirs, and interactions (the Coulomb interaction as well as the interaction between electron spin and nuclear spin) are essential for the entanglement generation. It is our purpose to discuss the entanglement generation in such an open system through an exact solution of scattering theory.

In this paper, we obtain an exact result for entanglement property of transported electrons of the two-lead Anderson model. The Anderson model is a fundamental model describing the electron transport through a quantum dot as illustrated in Fig. 1(a). It consists of a quantum dot with a single spin-degenerate level and two leads of noninteracting electrons each of which lead is coupled to the dot. There are four configurations in the quantum dot, i.e., empty, single occupation with an up spin or a down spin and double occupation with opposite spins. Among them, two electrons in the double occupation interact with each other (the Hubbard interaction). In order to describe an open system, we consider the single level with infinitely long leads rather than treating a quantum dot connected to large electron reservoirs. In this system, the electrons that enter from one lead are scattered by the quantum dot and are divided into the reflected wave on the same lead and the transmitted wave on the other lead. These scattered waves never come back to the dot again. The Landauer formula[9] tells us that this property captures a characteristics of a system with electron reservoirs.

We calculate the transition rate from the nonentangled two-electron incident state with momenta k_1 and k_2 on the lead 1 to the singlet and triplet states with momenta q_1 and q_2 on the lead 2. In the scattering process that conserves the set of momenta as in Fig. 1(b), both the triplet and the singlet components of the incident state can be transmitted to the lead 2. On the other hand, in the scattering process which conserves the total energy but not the set of momenta as in Fig. 1(c), we will find that only the singlet component can be transmitted and the triplet component is filtered out. The process in Fig. 1(c) represents that both two electrons with momenta k_1 and k_2 occupy the quantum dot during the same period, change their momenta to q_1 and q_2 due to the Coulomb interaction, and come out into the lead 2. In this paper, we call such a process a cotunneling process. (The term "cotunneling process" is often used for a tunneling process of a single electron in a specific order of perturbation theory. Here, we are using the term for a tunneling process of two electrons up to infinite order of the interaction parameter U.) We will clarify this mechanism by calculating the transition rates exactly, which is the main achievement of our approach. The mechanism of the entanglement generation was first proposed in Ref. 3; the lowest order of our result reproduces their perturbative result. Recently, a similar mechanism of entanglement generation is proposed in a side-coupled quantum dot[10] and an interaction-induced orbital entanglement property has been also discussed in a quantum-dot system.[11]

For the above purpose, we obtain the exact solution of the two-electron scattering state. A remarkable point of the state is that it contains a two-body singlet bound state. The bound

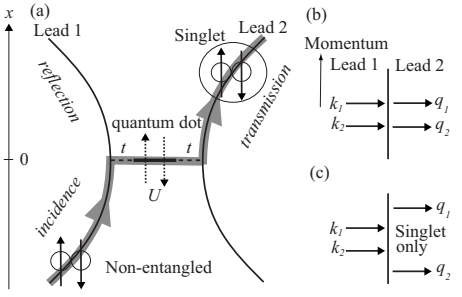

FIG. 1. (a) A schematic diagram of the Anderson model. (b) A scattering process that conserves the set of momenta. (c) A cotunneling process.

state is induced in the cotunneling process [Fig. 1(c)] by the Hubbard interaction on the quantum dot. A many-body eigenstate of the *closed* Anderson model can be constructed by the Bethe ansatz.[12–15] In contrast, our exact scattering state is a many-body eigenstate of the *open* Anderson model and essentially different from the Bethe eigenstate. A similar bound state is also discussed in Ref. 16, where the two-electron scattering matrix has been constructed exactly in the Anderson model. While their study is focused on the asymptotic states of electrons that lie far from the quantum dot, our exact solution describes electron states both inside and around the quantum dot.

The paper is organized as follows. In Sec. II, we give the definition of the two-lead Anderson model and present our main result. In order to obtain the result, we need to obtain the two-electron scattering state. The exact construction of this state is given in Sec. III. Concluding remarks are given in Sec. IV.

II. MODEL AND RESULT

A. Two-lead Anderson model

The Hamiltonian of the Anderson model is defined as $H=H_0+H_1$, where

$$H_0=\sum_k \sum_{\sigma=\uparrow,\downarrow} \sum_{\ell=1,2} \epsilon(k) c^\dagger_{\ell k\sigma} c_{\ell k\sigma} + \sum_{\sigma=\uparrow,\downarrow} \epsilon_d n_{d\sigma} + U n_{d\uparrow} n_{d\downarrow}, \tag{1}$$

$$H_1=\frac{t}{\sqrt{2}} \sum_k \sum_{\sigma=\uparrow,\downarrow} \sum_{\ell=1,2} (c^\dagger_{\ell k\sigma} d_\sigma + d^\dagger_\sigma c_{\ell k\sigma}). \tag{2}$$

Here, $c^\dagger_{\ell k\sigma}$ ($c_{\ell k\sigma}$) denotes the creation (annihilation) operator of an electron with momentum k and spin $\sigma(=\uparrow,\downarrow)$ on the lead $\ell(=1,2)$. Each lead is represented as a noninteracting Fermionic chain with the dispersion relation $\epsilon(k)$. The operator $d^\dagger_\sigma$ (d_σ) represents the creation (annihilation) operator of an electron on the quantum dot and $n_{d\sigma}=d^\dagger_\sigma d_\sigma$. We consider a single spin-degenerate level on the dot. When the energy level of the quantum dot is occupied by two electrons with opposite spins, they feel the Coulomb repulsion energy $U>0$. Thus, two effective energy levels on the dot are given by ϵ_d and ϵ_d+U. Depending on whether the levels are occupied by the electrons, there are four possible configurations; the empty state with total energy 0, a single occupation by an electron with either spin $\sigma(=\uparrow,\downarrow)$ with total energy ϵ_d, and the double occupation with total energy $2\epsilon_d+U$. The parameter t represents the coupling between each lead and the dot.

In this paper, we consider the model where the lead energy $\epsilon(k)$ is linearized in the vicinity of the Fermi energy to be $\epsilon(k)=\epsilon_F+v_F(k-k_F)$.[13–15] This assumption is valid when the other parameters t, ϵ_d, and U are small compared with the Fermi energy. Hereafter, we set $v_F=1$, $k_F=0$ and $\epsilon_F=0$ for simplicity without loss of generality. Under the assumption, the Hamiltonian above is transformed to the following model with continuous leads:

$$H_0=\sum_{\sigma=\uparrow,\downarrow} \sum_{\ell=1,2} \int_{-\infty}^{\infty} dx c^\dagger_{\ell\sigma}(x) \frac{1}{\mathrm{i}} \frac{d}{dx} c_{\ell\sigma}(x) + \sum_{\sigma=\uparrow,\downarrow} \epsilon_d n_{d\sigma} + U n_{d\uparrow} n_{d\downarrow}, \tag{3}$$

$$H_1=\frac{t}{\sqrt{2}} \sum_{\sigma=\uparrow,\downarrow} \sum_{\ell=1,2} [c^\dagger_{\ell\sigma}(0) d_\sigma + d^\dagger_\sigma c_{\ell\sigma}(0)]. \tag{4}$$

Here, the relation between the coordinate representation and the momentum representation is given by

$$c^\dagger_{\ell k\sigma}=\frac{1}{\sqrt{2\pi}} \int dx e^{\mathrm{i}kx} c^\dagger_{\ell\sigma}(x), \quad c_{\ell k\sigma}=\frac{1}{\sqrt{2\pi}} \int dx e^{-\mathrm{i}kx} c_{\ell\sigma}(x). \tag{5}$$

Note that there are only right-moving electrons on the leads since we have set $v_F=1$ in the linearized dispersion relation. Even in this situation, we can take both reflection and transmission modes into account; when we regard the region $x<0$ on the lead 1 as the incident mode, the regions $x>0$ on the lead 1 and 2 can be interpreted as the reflection and the transmission modes, respectively [see Fig. 1(a)]. This "unfolded" picture was also explained in Ref. 17.

In the model described by Eqs. (3) and (4), we consider the situation studied in Ref. 3. Let $|k_1,k_2;1\rangle$ be the nonentangled incident state with momenta k_1 and k_2 on the lead 1 defined by

$$|k_1,k_2;1\rangle^{(\mathrm{i})}=c^\dagger_{1k_1\uparrow} c^\dagger_{1k_2\downarrow} |0\rangle, \tag{6}$$

where $|0\rangle$ denotes the vacuum state. We also define a triplet state $|q_1,q_2;2,+\rangle^{(\mathrm{f})}$ and a singlet state $|q_1,q_2;2,-\rangle^{(\mathrm{f})}$ with momenta q_1 and q_2 on the lead 2,

$$|q_1,q_2;2,\pm\rangle^{(\mathrm{f})}=\frac{1}{\sqrt{2}} (c^\dagger_{2q_1\uparrow} c^\dagger_{2q_2\downarrow} \pm c^\dagger_{2q_1\downarrow} c^\dagger_{2q_2\uparrow}) |0\rangle, \tag{7}$$

which are used as outgoing states. Our purpose is to calculate the transition amplitude between these states,

$${}^{(\mathrm{f})}\langle q_1,q_2;2,\pm|T(E_k)|k_1,k_2;1\rangle^{(\mathrm{i})} \delta(E_k-E_q), \tag{8}$$

where $E_k=k_1+k_2$, $E_q=q_1+q_2$ and $T(E)$ represents the transition matrix defined by the recursion relation

$$T(E)=H_1+H_1\frac{1}{E-H_0+\mathrm{i}0} T(E). \tag{9}$$

The definition is originated from the Lippmann-Schwinger equation, Eq. (15), which will be described in Sec. III A.

B. Main result

We will obtain new exact results for the transition amplitudes

$$\begin{aligned} &{}^{(\mathrm{f})}\langle q_1,q_2;2,+|T(E_k)|k_1,k_2;1\rangle^{(\mathrm{i})} \delta(E_k-E_q) \\ &=\frac{t^2 e_{k_1} e_{k_2}}{4\sqrt{2}\mathrm{i}} (\delta(k_1-q_1)\delta(k_2-q_2)-\delta(k_1-q_2)\delta(k_2-q_1)), \end{aligned} \tag{10}$$

$$
\begin{aligned}
&{}^{(\mathrm{f})}\langle q_1,q_2;2,-|T(E_k)|k_1,k_2;1\rangle^{(\mathrm{i})}\delta(E_k-E_q)\\
&=\frac{t^2 e_{k_1}e_{k_2}}{4\sqrt{2}\mathrm{i}}(\delta(k_1-q_1)\delta(k_2-q_2)+\delta(k_1-q_2)\delta(k_2-q_1))\\
&\quad+\frac{U}{2\sqrt{2}}\frac{E_k-2\epsilon_d+\mathrm{i}t^2}{E_k-2\epsilon_d-U+\mathrm{i}t^2}e_{k_1}e_{k_2}e_{q_1}e_{q_2}\delta(E_k-E_q),
\end{aligned}
\tag{11}
$$

where e_k is defined in Eq. (25) below. Equation (10) and the first term in Eq. (11) represent the contributions from the scattering process which conserves the set of momenta $\{k_1,k_2\}=\{q_1,q_2\}$ as shown in Fig. 1(b). Note that they vanish if k_i and q_j satisfy the condition of the cotunneling process [Fig. 1(c)],

$$
E_k=E_q,\quad \{k_1,k_2\}\neq\{q_1,q_2\}. \tag{12}
$$

In contrast, Eq. (11) has an additional term, which remains nonzero for $U>0$ under the condition (12). The contribution appears only in the transition into the singlet state [Eq. (11)], not in the transition into the triplet state [Eq. (10)]. In other words, we will observe only singlet states if we wait for outgoing electrons on the lead 2 under the condition (12).

Figure 2 shows the dependence of the transition rate $2\pi|{}^{(\mathrm{f})}\langle q_1,q_2;2,-|T(E_k)|k_1,k_2;1\rangle^{(\mathrm{i})}|^2$ on the interaction energy U for $t<E_k$ [Fig. 2(a)] and $t>E_k$ [Fig. 2(b)]. The solid lines indicate our exact result and the dashed lines represent the perturbative result in the lowest order of t,

$$
{}^{(\mathrm{f})}\langle q_1,q_2;2,+|T(E_k)|k_1,k_2;1\rangle^{(\mathrm{i})}\delta(E_k-E_q)=\frac{t^4}{8\sqrt{2}\pi\mathrm{i}(k_1-\epsilon_d)(k_2-\epsilon_d)}(\delta(k_1-q_1)\delta(k_2-q_2)-\delta(k_1-q_2)\delta(k_2-q_1))+O(t^6), \tag{13}
$$

$$
\begin{aligned}
{}^{(\mathrm{f})}\langle q_1,q_2;2,-|T(E_k)|k_1,k_2;1\rangle^{(\mathrm{i})}\delta(E_k-E_q)&=\frac{t^4}{8\sqrt{2}\pi\mathrm{i}(k_1-\epsilon_d)(k_2-\epsilon_d)}(\delta(k_1-q_1)\delta(k_2-q_2)+\delta(k_1-q_2)\delta(k_2-q_1))\\
&\quad+\frac{U(E_k-2\epsilon_d)}{8\sqrt{2}\pi^2(E_k-2\epsilon_d-U)(k_1-\epsilon_d)(k_2-\epsilon_d)(q_1-\epsilon_d)(q_2-\epsilon_d)}\delta(E_k-E_q)+O(t^6)
\end{aligned}
\tag{14}
$$

which was obtained in Ref. 3. The perturbative one, being divergent, fails when $U\simeq E_k$ even for $t<E_k$.

III. ONE- AND TWO-ELECTRON SCATTERING STATES

A. Lippmann-Schwinger equation

We consider the scattering state $|\phi\rangle$ given by the solution of the Lippmann-Schwinger equation,

$$
|\phi\rangle=|\phi\rangle^{(\mathrm{i})}+\frac{1}{E-H_0+\mathrm{i}0}H_1|\phi\rangle, \tag{15}
$$

where $|\phi\rangle^{(\mathrm{i})}$ denotes an incident state which satisfies $H_0|\phi\rangle^{(\mathrm{i})}=E|\phi\rangle^{(\mathrm{i})}$. The definition (9) of the transition matrix $T(E)$ is originated from the relation $T(E)|\phi\rangle^{(\mathrm{i})}=H_1|\phi\rangle$ with the solution $|\phi\rangle$. We are particularly interested in the two-electron scattering state $|k_1,k_2;1\rangle$, which is the solution of Eq. (15) with $|\phi\rangle^{(\mathrm{i})}=|k_1,k_2;1\rangle^{(\mathrm{i})}$ given by Eq. (6) and $E=E_k=k_1+k_2$. The transition amplitude (8) is then expressed in the form

$$
{}^{(\mathrm{f})}\langle q_1,q_2;2,\pm|T(E_k)|k_1,k_2;1\rangle^{(\mathrm{i})}={}^{(\mathrm{f})}\langle q_1,q_2;2,\pm|H_1|k_1,k_2;1\rangle. \tag{16}
$$

In this section, we will construct the exact solution of the state $|k_1,k_2;1\rangle$. We start our discussion by introducing the even-odd transformation, which turns the two-lead Anderson model into a simpler form. In Ref. 18, we applied the same technique to a spinless model and obtained the exact solution of many-electron scattering states.

The even-odd transformation is defined by

$$
c_{e\sigma}(x)=\frac{1}{\sqrt{2}}[c_{1\sigma}(x)+c_{2\sigma}(x)],
$$

$$
c_{o\sigma}(x)=\frac{1}{\sqrt{2}}[c_{1\sigma}(x)-c_{2\sigma}(x)]. \tag{17}
$$

Applying this transformation to the two-lead Anderson model (3) and (4), we decompose the Hamiltonian into $H=H_e+H_o$, where

$$
\begin{aligned}
H_e&=\sum_{\sigma=\uparrow,\downarrow}\left[\int dx c_{e\sigma}^{\dagger}(x)\frac{1}{\mathrm{i}}\frac{d}{dx}c_{e\sigma}(x)+\epsilon_d n_{d\sigma}\right]+Un_{d\uparrow}n_{d\downarrow}\\
&\quad+\sum_{\sigma=\uparrow,\downarrow}t[c_{e\sigma}^{\dagger}(0)d_{\sigma}+d_{\sigma}^{\dagger}c_{e\sigma}(0)],
\end{aligned}
\tag{18}
$$

$$
H_o=\sum_{\sigma=\uparrow,\downarrow}\int dx c_{o\sigma}^{\dagger}(x)\frac{1}{\mathrm{i}}\frac{d}{dx}c_{o\sigma}(x). \tag{19}
$$

Note that the odd part H_o is completely decoupled from the even part H_e. Thus, the two-lead Anderson model (3) and (4)

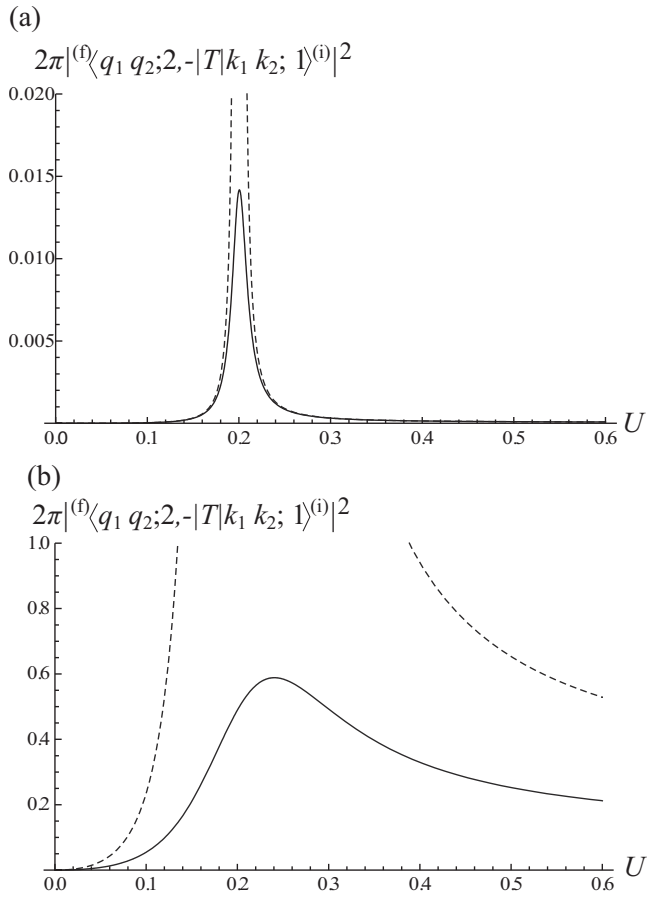

FIG. 2. The transition rate $2\pi|^{(f)}\langle q_1,q_2;2,-|T(E_k)|k_1,k_2;1\rangle^{(i)}|^2$ obtained from our exact solution (solid line) and a perturbative one (dashed line) for $\epsilon_d=0$, $k_1=k_2=0.1$, $q_1=0.05$, $q_2=0.15$, $E_k=E_q=0.2$ with (a) $t=0.1(<E_k)$ and (b) $t=0.3(>E_k)$.

can be transformed to the one-lead Anderson model (18) with the free part (19).

Through the even-odd transformation, the scattering state $|k_1,k_2;1\rangle$ is expressed as[18]

$$|k_1,k_2;1\rangle = \frac{1}{2}(|k_1,k_2\rangle_{ee} + |k_1,k_2\rangle_{eo} + |k_1,k_2\rangle_{oe} + |k_1,k_2\rangle_{oo}), \tag{20}$$

where $|k_1,k_2\rangle_{\alpha\beta}$ $[(\alpha,\beta)=(e,e),(e,o),(o,e),(o,o)]$ denotes the solution of the Lippmann-Schwinger equation (15) with the incident state $|\phi\rangle^{(i)}=|k_1,k_2\rangle^{(i)}_{\alpha\beta}:=c^\dagger_{\alpha k_1\uparrow}c^\dagger_{\beta k_2\downarrow}|0\rangle$. We note that $H_0|k_1,k_2\rangle^{(i)}_{\alpha\beta}=E_k|k_1,k_2\rangle^{(i)}_{\alpha\beta}$.

B. One-electron scattering states

Before giving these two-electron scattering eigenstates, we first consider the tutorial case of the one-electron eigenstate $|k\sigma;1\rangle$ $(\sigma=\uparrow,\downarrow)$, which is the solution of Eq. (15) with $|\phi\rangle^{(i)}=c^\dagger_{1k\sigma}|0\rangle$ and $E=k$. After the even-odd transformation (17), the scattering state is written as

$$|k\sigma;1\rangle = \frac{1}{\sqrt{2}}(|k\sigma\rangle_e + |k\sigma\rangle_o), \tag{21}$$

where $|k\sigma\rangle_\alpha$ ($\alpha=e,o$ and $\sigma=\uparrow,\downarrow$) is the one-electron scattering state (15) with $|\phi\rangle^{(i)}=c^\dagger_{\alpha k\sigma}|0\rangle$. The one-electron eigenstates can be expressed as follows:

$$|k\sigma\rangle_e = \left(\int dx g_k(x)c^\dagger_{e\sigma}(x) + e_k d^\dagger_\sigma\right)|0\rangle, \tag{22}$$

$$|k\sigma\rangle_o = \int dx h_k(x)c^\dagger_{o\sigma}(x)|0\rangle, \tag{23}$$

where the eigenfunctions are given by

$$g_k(x) = \frac{1}{\sqrt{2\pi}}e^{ikx}(\theta(-x) + \theta(x)e^{i\delta_k}), \tag{24}$$

$$e_k = \frac{1}{\sqrt{2\pi}}\frac{t}{k-\epsilon_d+it^2/2}, \quad h_k(x) = \frac{1}{\sqrt{2\pi}}e^{ikx}. \tag{25}$$

Here, $\theta(x)$ is the step function with $\theta(0)=1/2$ and $e^{i\delta_k}:=e_k/e_k^*$ in Eq. (24) represents the phase factor due to the scattering at the dot.

The derivation of these eigenfunctions is as follows. For the odd part, we can easily find that $h_k(x)$ in Eq. (23) is the plane wave presented in Eq. (25) since the Hamiltonian (19) is completely free. For the even part, the Schrödinger equation $H_e|k\sigma\rangle_e=k|k\sigma\rangle_e$ reads

$$\frac{1}{i}(\partial_x - k)g_k(x) + t\delta(x)e_k = 0, \tag{26}$$

$$(\epsilon_d - k)e_k + tg_k(0) = 0. \tag{27}$$

In the case $x\neq 0$, the function $g_k(x)$ is just a plane wave. Due to the δ-function term in Eq. (26), $g_k(x)$ is discontinuous at $x=0$. Since the value $g_k(0)$ is not determined by the Schrödinger equations, we assume

$$g_k(0) = \frac{1}{2}[g_k(0-) + g_k(0+)]. \tag{28}$$

The discontinuity of $g_k(x)$ is characterized by the following matching condition:

$$g_k(0+) - g_k(0-) = -ite_k, \tag{29}$$

which is obtained by integrating Eq. (26) from $-\epsilon$ to ϵ and taking the limit $\epsilon\to 0$. From Eqs. (27) and (29) with Eq. (28), we find

$$e_k = \frac{t}{k-\epsilon_d+it^2/2}g_k(0-), \quad g_k(0+) = e^{i\delta_k}g_k(0-). \tag{30}$$

Thus, we obtain the eigenfunctions (24) and (25). The constant factor $g_k(0-)$ is determined to be $1/\sqrt{2\pi}$ by the normalization condition ${}_e\langle k\sigma|k'\sigma'\rangle_e=\delta(k-k')\delta_{\sigma\sigma'}$.

C. Two-electron scattering states

Next, extending the calculation for the one-electron scattering state, we consider the two-electron scattering states

$|k_1,k_2\rangle_{\alpha\beta}$ $[(\alpha,\beta)=(e,e),(e,o),(o,e),(o,o)]$. These can be written in the forms

$$|k_1,k_2\rangle_{ee}=\left(\int dx_1dx_2g_{ee}(x_1,x_2)c^\dagger_{e\uparrow}(x_1)c^\dagger_{e\downarrow}(x_2)+\int dxe_{\uparrow ee}(x)c^\dagger_{e\downarrow}(x)d^\dagger_\uparrow+\int dxe_{\downarrow ee}(x)c^\dagger_{e\uparrow}(x)d^\dagger_\downarrow+f_{ee}d^\dagger_\uparrow d^\dagger_\downarrow\right)|0\rangle, \tag{31}$$

$$|k_1,k_2\rangle_{eo}=\left(\int dx_1dx_2g_{eo}(x_1,x_2)c^\dagger_{e\uparrow}(x_1)c^\dagger_{o\downarrow}(x_2)+\int dxe_{\uparrow eo}(x)c^\dagger_{o\downarrow}(x)d^\dagger_\uparrow\right)|0\rangle, \tag{32}$$

$$|k_1,k_2\rangle_{oe}=\left(\int dx_1dx_2g_{oe}(x_1,x_2)c^\dagger_{o\uparrow}(x_1)c^\dagger_{e\downarrow}(x_2)+\int dxe_{\downarrow oe}(x)c^\dagger_{o\uparrow}(x)d^\dagger_\downarrow\right)|0\rangle, \tag{33}$$

$$|k_1,k_2\rangle_{oo}=\int dx_1dx_2g_{oo}(x_1,x_2)c^\dagger_{o\uparrow}(x_1)c^\dagger_{o\downarrow}(x_2)|0\rangle. \tag{34}$$

For the cases except $\alpha=\beta=e$, the scattering states are free of the Coulomb interaction U because the even and odd Hamiltonians (18) and (19) are completely decoupled. Thus, the eigenfunctions are given by the products of the one-electron eigenfunctions (24) and (25) as

$$g_{eo}(x_1,x_2)=g_{k_1}(x_1)h_{k_2}(x_2),\quad e_{\uparrow eo}(x)=-e_{k_1}h_{k_2}(x),$$

$$g_{oe}(x_1,x_2)=h_{k_1}(x_1)g_{k_2}(x_2),\quad e_{\downarrow oe}(x)=e_{k_2}h_{k_1}(x),$$

$$g_{oo}(x_1,x_2)=h_{k_1}(x_1)h_{k_2}(x_2). \tag{35}$$

Let us now consider the case $\alpha=\beta=e$. Only in this case, the eigenfunctions depend on the interaction U. These are given as follows:

$$g_{ee}(x_1,x_2)=g_{k_1}(x_1)g_{k_2}(x_2)+e^{iE_kx_2}\theta(x_1)Z(x_1-x_2)+e^{iE_kx_1}\theta(x_2)Z(x_2-x_1), \tag{36}$$

$$e_{\uparrow ee}(x)=-e_{k_1}g_{k_2}(x)-\frac{i}{t}e^{iE_kx}Z(-x), \tag{37}$$

$$e_{\downarrow ee}(x)=e_{k_2}g_{k_1}(x)+\frac{i}{t}e^{iE_kx}Z(-x), \tag{38}$$

$$f_{ee}=e_{k_1}e_{k_2}-\frac{2}{t^2}Z(0), \tag{39}$$

where $E_k=k_1+k_2$ and

$$Z(x)=\frac{-t^2Ue_{k_1}e_{k_2}}{E_k-2\epsilon_d-U+it^2}e^{i(\epsilon_d-it^2/2)x}\theta(-x). \tag{40}$$

In Eqs. (36)–(39), the function $Z(x)$ describes an effect of the interaction. The derivation of these results will be given in the next subsection.

From Eqs. (16), (20), and (31)–(34), we find that the transition amplitude (8) is expressed as

$$^{(f)}\langle q_1,q_2;2,\pm|T(E_k)|k_1,k_2;1\rangle^{(i)}\delta(E_k-E_q)=\frac{t}{8\sqrt{\pi}}\int dx[h^*_{q_2}(x)\mp h^*_{q_1}(x)]\{[e_{\uparrow eo}(x)-e_{\uparrow ee}(x)]\pm[e_{\downarrow oe}(x)-e_{\downarrow ee}(x)]\}\delta(E_k-E_q) \tag{41}$$

where $h_k(x)$ is defined by Eq. (25). Thus, substituting the results on $e_{\sigma\alpha\beta}(x)$ in Eqs. (35), (37), and (38) into this equation, we obtain the exact transition amplitudes (10) and (11).

Remarkable is that Eqs. (36)–(38) contain the term $Z(x)$, Eq. (40), which represents a *two-body bound state*. The range of binding is t^{-2}, which itself is independent of U. Note the following properties:

(i) the bound state is induced by the Coulomb interaction U; it vanishes for $U=0$. It describes the process where both electrons with opposite spins are on the dot. In order for the two electrons to interact, in a short period during which the first electron stays on the dot, the second electron has to come into the dot. Therefore, we can expect that the longer the distance between the two electrons is, the smaller the probability of observing such a process. The exponential decay in the bound state represents this situation.

(ii) The bound state appears in the cotunneling process (12), which is a scattering process that does not conserve the momentum set. In contrast, the first term of Eq. (36) represents the direct $(k_1=q_1,k_2=q_2)$ and exchange $(k_1=q_2,k_2=q_1)$ processes.

(iii) The bound state appears only in the case $\alpha=\beta=e$ since the term $d^\dagger_\uparrow d^\dagger_\downarrow|0\rangle$ does not exist in the other cases and thereby the eigenfunctions do not depend on U.

From these properties, we find that it is this bound state that produces the second term of the transition rate to the singlet state in Eq. (11).

These scattering states (35)–(40) are important for the study of transport properties in the *open* quantum system. In a *closed* system with a periodic boundary condition, the exact eigenfunctions in the Anderson model were obtained by the Bethe ansatz.[12–15] Our results (36)–(40) are essentially different from the Bethe eigenstates. In the Bethe ansatz, $g_{ee}(x_1,x_2)$ would be in the following form:

$$g_{ee}(x_1,x_2)=\sum_Q A_Qg_{k_1}(x_{Q_1})g_{k_2}(x_{Q_2}). \tag{42}$$

Here, $Q=(1,2),(2,1)$ and A_Q depends on k_i and the parameters of the model, i.e., ϵ_d, t and U. Note that the solution is characterized by the fixed set $\{k_1,k_2\}$. Although k_i could be a complex number, it is obvious that Eq. (42) cannot describe the form of Eq. (36).

D. Proof of Eqs. (36)–(40)

We now present the derivation of the two-electron wave functions (36)–(40). The scattering eigenstate $|k_1,k_2\rangle_{ee}$ is obtained by solving the two-electron Schrödinger equation $H_e|k_1,k_2\rangle_{ee}=E_k|k_1,k_2\rangle_{ee}$, which reads

$$\left(\frac{1}{\mathrm{i}}(\partial_1+\partial_2)-E_k\right)g_{ee}(x_1,x_2)+t(\delta(x_2)e_{\downarrow ee}(x_1)-\delta(x_1)e_{\uparrow ee}(x_2))=0, \tag{43}$$

$$\left(\frac{1}{\mathrm{i}}\partial_x+\varepsilon_d-E_k\right)e_{\uparrow ee}(x)-tg_{ee}(0,x)-t\delta(x)f_{ee}=0, \tag{44}$$

$$\left(\frac{1}{\mathrm{i}}\partial_x+\varepsilon_d-E_k\right)e_{\downarrow ee}(x)+tg_{ee}(x,0)+t\delta(x)f_{ee}=0, \tag{45}$$

$$(E_k-2\epsilon_d-U)f_{ee}-t[e_{\downarrow ee}(0)-e_{\uparrow ee}(0)]=0, \tag{46}$$

where $E_k=k_1+k_2$. As in Eq. (28), we set

$$g_{ee}(0,x)=\frac{1}{2}[g_{ee}(0-,x)+g_{ee}(0+,x)], \tag{47}$$

$$g_{ee}(x,0)=\frac{1}{2}[g_{ee}(x,0-)+g_{ee}(x,0+)], \tag{48}$$

$$e_{\sigma ee}(0)=\frac{1}{2}[e_{\sigma ee}(0-)+e_{\sigma ee}(0+)] \tag{49}$$

for $\sigma=\uparrow,\downarrow$. The boundary condition is

$$g_{ee}(x_1,x_2)=\frac{1}{2\pi}e^{\mathrm{i}(k_1x_1+k_2x_2)}, \tag{50}$$

for $x_1, x_2<0$. It is obvious that the eigenfunction (36) satisfies this condition. Note that the condition corresponds to the plane-wave incident state $|k_1,k_2\rangle_{ee}^{(\mathrm{i})}=c_{ek_1\uparrow}^{\dagger}c_{ek_2\downarrow}^{\dagger}|0\rangle$. Indeed, we can directly confirm that our solution (36)–(40) of the Schrödinger equations (43)–(46) satisfies the Lippmann-Schwinger equation (15) with $|\phi\rangle^{(\mathrm{i})}=|k_1,k_2\rangle_{ee}^{(\mathrm{i})}$.

We rewrite the set of the equations in more convenient forms, that is, matching conditions and the differential equations without the δ-function terms. Integrating each variable of Eqs. (43)–(46) from $-\epsilon$ to ϵ and taking $\epsilon\to 0$, we obtain the following matching conditions, which describe the discontinuities of the eigenfunctions:

$$g_{ee}(0+,x)-g_{ee}(0-,x)=\mathrm{i}te_{\uparrow ee}(x), \tag{51}$$

$$g_{ee}(x,0+)-g_{ee}(x,0-)=-\mathrm{i}te_{\downarrow ee}(x), \tag{52}$$

$$e_{\uparrow ee}(0+)-e_{\uparrow ee}(0-)=\mathrm{i}tf_{ee}, \tag{53}$$

$$e_{\downarrow ee}(0+)-e_{\downarrow ee}(0-)=-\mathrm{i}tf_{ee}. \tag{54}$$

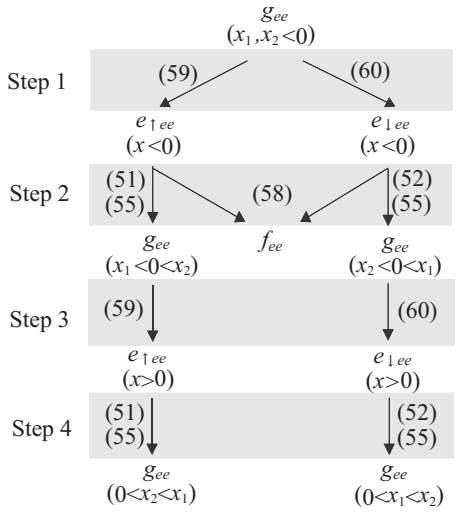

FIG. 3. Flow chart for constructing the two-electron scattering state $|k_1,k_2\rangle_{ee}$. Our starting point (50) is represented on the top. Near each arrow, we describe the number(s) of equation(s) that we use to obtain respective target.

Then, through the conditions, the Schrödinger equations for $x_1\neq 0$, $x_2\neq 0$, and $x\neq 0$ are written as

$$(\partial_1+\partial_2)g_{ee}(x_1,x_2)=\mathrm{i}E_kg_{ee}(x_1,x_2), \tag{55}$$

$$\partial_x e_{\uparrow ee}(x)=\mathrm{i}\left(E_k-\epsilon_d+\frac{\mathrm{i}t^2}{2}\right)e_{\uparrow ee}(x)+\mathrm{i}tg_{ee}(0-,x), \tag{56}$$

$$\partial_x e_{\downarrow ee}(x)=\mathrm{i}\left(E_k-\epsilon_d+\frac{\mathrm{i}t^2}{2}\right)e_{\downarrow ee}(x)-\mathrm{i}tg_{ee}(x,0-), \tag{57}$$

$$(E_k-2\epsilon_d-U+\mathrm{i}t^2)f_{ee}=t[e_{\downarrow ee}(0-)-e_{\uparrow ee}(0-)]. \tag{58}$$

Since Eqs. (56) and (57) are first-order differential equations, we can readily integrate them. We have

$$e_{\uparrow ee}(x)=B_re^{\mathrm{i}(E_k-\epsilon_d+\mathrm{i}t^2/2)x}+\mathrm{i}te^{\mathrm{i}(E_k-\epsilon_d+\mathrm{i}t^2/2)x}\int_{c_r}^{x}dye^{-\mathrm{i}(E_k-\epsilon_d+\mathrm{i}t^2/2)y}g_{ee}(0-,y), \tag{59}$$

$$e_{\downarrow ee}(x)=C_re^{\mathrm{i}(E_k-\epsilon_d+\mathrm{i}t^2/2)x}-\mathrm{i}te^{\mathrm{i}(E_k-\epsilon_d+\mathrm{i}t^2/2)x}\int_{c_r}^{x}dye^{-\mathrm{i}(E_k-\epsilon_d+\mathrm{i}t^2/2)y}g_{ee}(y,0-), \tag{60}$$

where $c_{\mathrm{I}}=-\infty$ and $c_{\mathrm{II}}=0$. The constants B_r and C_r are constants of integration, which may be different in the regions $r=\mathrm{I}(x<0)$ and $\mathrm{II}(x>0)$.

In the following, we use Eqs. (51), (52), (55), and (58)–(60) in place of the original Schrödinger equations (43)–(46). Starting from Eq. (50), we construct the eigenfunctions in the order described in the flow chart Fig. 3.

1. Step 1

We find $B_{\mathrm{I}}=C_{\mathrm{I}}=0$, or the first terms in Eqs. (59) and (60), would be divergent as $x\to-\infty$. Thus, from Eq. (59) with Eq. (50), we have

$$e_{\uparrow ee}(x)=-\frac{e_{k_1}}{\sqrt{2\pi}}e^{\mathrm{i}k_2x}\ \text{ for }\ x<0. \tag{61}$$

Here, e_k is given by Eq. (25). Similarly from Eq. (60) with Eq. (50), we have

$$e_{\downarrow ee}(x)=\frac{e_{k_2}}{\sqrt{2\pi}}e^{\mathrm{i}k_1x}\ \text{ for }\ x<0. \tag{62}$$

2. Step 2

From the matching condition (51) with Eqs. (50) and (61), we find

$$g_{ee}(0+,x)=\frac{1}{2\pi}e^{\mathrm{i}(k_2x+\delta_{k_1})}\ \text{ for }\ x<0, \tag{63}$$

where $e^{\mathrm{i}\delta_k}$ represents the phase factor appearing in the one-electron scattering state (24). Dependence of the eigenfunction on the first variable can be recovered from Eq. (55),

$$g_{ee}(x_1,x_2)=\frac{1}{2\pi}e^{\mathrm{i}(k_1x_1+k_2x_2+\delta_{k_1})}\ \text{ for }\ x_2<0<x_1. \tag{64}$$

Similarly, using the matching condition (52) with Eqs. (50) and (62), we find

$$g_{ee}(x_1,x_2)=\frac{1}{2\pi}e^{\mathrm{i}(k_1x_1+k_2x_2+\delta_{k_2})}\ \text{ for }\ x_1<0<x_2. \tag{65}$$

Furthermore, substituting Eqs. (61) and (62) into Eq. (58), we obtain the result for f_{ee}, Eq. (39).

3. Step 3

From Eqs. (59) with Eq. (65), we have

$$e_{\uparrow ee}(x)=\tilde{B}_{\mathrm{II}}e^{\mathrm{i}(E_k-\epsilon_d+\mathrm{i}t^2/2)x}-\frac{e_{k_1}}{\sqrt{2\pi}}e^{\mathrm{i}(k_2x+\delta_{k_2})}\ \text{ for }\ x>0, \tag{66}$$

where $\tilde{B}_{\mathrm{II}}=B_{\mathrm{II}}+e_{k_1}e^{\mathrm{i}\delta_{k_2}}/\sqrt{2\pi}$. Note that the first term in this equation does not appear in Eq. (61). This term produces the function $Z(-x)$, Eq. (40). The coefficient is determined by the matching condition (53) with Eqs. (39) and (61),

$$\tilde{B}_{\mathrm{II}}=\frac{\mathrm{i}tUe_{k_1}e_{k_2}}{E_k-2\epsilon_d-U+\mathrm{i}t^2}. \tag{67}$$

Similarly, we obtain

$$e_{\downarrow ee}(x)=\frac{-\mathrm{i}tUe_{k_1}e_{k_2}}{E_k-2\epsilon_d-U+\mathrm{i}t^2}e^{\mathrm{i}(E_k-\epsilon_d+\mathrm{i}t^2/2)x}+\frac{e_{k_2}}{\sqrt{2\pi}}e^{\mathrm{i}(k_1x+\delta_{k_1})}\quad\text{for }\ x>0. \tag{68}$$

4. Step 4

Following the same procedure as Step 2 with the results (66)–(68), we have

$$g_{ee}(x_1,x_2)=-\frac{t^2U}{E_k-2\epsilon_d-U+\mathrm{i}t^2}e^{\mathrm{i}(E_kx_2-(\epsilon_d-\mathrm{i}t^2/2)(x_2-x_1))}+\frac{1}{2\pi}e^{\mathrm{i}(k_1x_1+k_2x_2+\delta_{k_1}+\delta_{k_2})} \tag{69}$$

for $0<x_1<x_2$ and

$$g_{ee}(x_1,x_2)=-\frac{t^2U}{E_k-2\epsilon_d-U+\mathrm{i}t^2}e^{\mathrm{i}(E_kx_1-(\epsilon_d-\mathrm{i}t^2/2)(x_1-x_2))}+\frac{1}{2\pi}e^{\mathrm{i}(k_1x_1+k_2x_2+\delta_{k_1}+\delta_{k_2})} \tag{70}$$

for $0<x_2<x_1$.

Summarizing the results obtained by these steps, we arrive at the desired expressions (36)–(39).

IV. CONCLUDING REMARKS

In this paper, we have constructed the exact two-electron scattering state and discussed its entanglement property. For the exact calculation of the transition rates (10) and (11), our solution is essential. We have clarified that the electron transport through the quantum dot has a potential advantage for entanglement generation.

One of the interesting problems in the future is how this two-particle entanglement can be extracted from the current through mesoscopic devices. In an open quantum dot system, the transport property depends on the temperature of the system.[19] When the temperature is higher than the Kondo temperature T_K, the sequential tunneling for electrons due to the Coulomb blockade becomes dominant. In this regime, coherence between electrons vanishes. In contrast, when the temperature is sufficiently low compared with T_K, the Kondo effect becomes prominent. Since the Kondo state is a singlet state of electrons in and out of the dot, this low-temperature regime can be advantageous for extraction of the entanglement discussed in this paper.

Our exact scattering state may also be a tool for understanding nonequilibrium electron transport of mesoscopic devices under a finite bias voltage. In a spinless model, the analytic approach for this topic has been proposed[20–23] and the importance of many-electron scattering states on the nonequilibrium current has been pointed out recently.[18,24,25] In particular, our approach in Ref. 18 succeeded in obtaining nonperturbative result on nonlinear current-voltage characteristics. Furthermore, for the Anderson model, nonequilibrium transport properties has been vigorously studied by perturbative[26,27] and numerical[28–30] approaches. We believe that our exact many-electron scattering state clarifies nonperturbative aspect of the Kondo effect out of equilibrium.[31–33]

ACKNOWLEDGMENTS

The authors would like to thank T. Fujii and G. Ordonez for discussions. One of the authors (T.I.) also would like to thank Y. Yamamoto for helpful comments. The present study is partially supported by CREST of Japan Science and Technology Agency, Grant-in-Aid for Young Scientists (B) under Grant No. 20740217 and Grant-in-Aid for Scientific Research (B) under Grant No. 17340115.

*Present address: Research Center for Advanced Science and Technology, The University of Tokyo, 4-6-1 Komaba, Meguro, 153-8904 Tokyo; timamura@iis.u-tokyo.ac.jp

†nishino@iis.u-tokyo.ac.jp

‡hatano@iis.u-tokyo.ac.jp

[1] M. Nielsen and I. Chuang, *Quantum Computation and Quantum Information* (Cambridge University Press, Cambridge, England, 2005).

[2] L. Amico, R. Fazio, A. Osterloh, and V. Vedral, Rev. Mod. Phys. **80**, 517 (2008).

[3] W. D. Oliver, F. Yamaguchi, and Y. Yamamoto, Phys. Rev. Lett. **88**, 037901 (2002).

[4] D. S. Saraga and D. Loss, Phys. Rev. Lett. **90**, 166803 (2003).

[5] A. V. Lebedev, G. Blatter, C. W. J. Beenakker, and G. B. Lesovik, Phys. Rev. B **69**, 235312 (2004).

[6] P. Samuelsson, E. V. Sukhorukov, and M. Büttiker, Phys. Rev. Lett. **92**, 026805 (2004).

[7] I. Neder, N. Ofek, Y. Chung, M. Heiblum, D. Mahalu, and V. Umansky, Nature (London) **448**, 333 (2007).

[8] H. Christ, J. I. Cirac, and G. Giedke, Phys. Rev. B **78**, 125314 (2008).

[9] S. Datta, *Electronic Transport in Mesoscopic Systems* (Cambridge University Press, Cambridge, England, 1995).

[10] D. Roy, Phys. Rev. B **80**, 245304 (2009).

[11] A. V. Lebedev, G. B. Lesovik, and G. Blatter, Phys. Rev. Lett. **100**, 226805 (2008).

[12] N. Andrei, Phys. Rev. Lett. **45**, 379 (1980).

[13] P. B. Wiegmann, Phys. Lett. A **80**, 163 (1980).

[14] N. Kawakami and A. Okiji, Phys. Lett. A **86**, 483 (1981).

[15] N. Kawakami and A. Okiji, J. Phys. Soc. Jpn. **51**, 1145 (1982).

[16] J. Shen and S. Fan, New J. Phys. **11**, 113024 (2009).

[17] R. M. Konik, H. Saleur, and A. W. W. Ludwig, Phys. Rev. B **66**, 125304 (2002).

[18] A. Nishino, T. Imamura, and N. Hatano, Phys. Rev. Lett. **102**, 146803 (2009).

[19] M. Pustilnik and L. I. Glazman, J. Phys.: Condens. Matter **16**, R513 (2004).

[20] P. Mehta and N. Andrei, Phys. Rev. Lett. **96**, 216802 (2006).

[21] A. Nishino and N. Hatano, J. Phys. Soc. Jpn. **76**, 063002 (2007).

[22] B. Doyon, Phys. Rev. Lett. **99**, 076806 (2007).

[23] E. Boulat and H. Saleur, Phys. Rev. B **77**, 033409 (2008).

[24] A. Dhar, D. Sen, and D. Roy, Phys. Rev. Lett. **101**, 066805 (2008).

[25] D. Roy, A. Soori, D. Sen, and A. Dhar, Phys. Rev. B **80**, 075302 (2009).

[26] S. Hershfield, J. H. Davies, and J. W. Wilkins, Phys. Rev. Lett. **67**, 3720 (1991).

[27] T. Fujii and K. Ueda, Phys. Rev. B **68**, 155310 (2003).

[28] S. Kirino, T. Fujii, J. Zhao, and K. Ueda, J. Phys. Soc. Jpn. **77**, 084704 (2008).

[29] S. Weiss, J. Eckel, M. Thorwart, and R. Egger, Phys. Rev. B **77**, 195316 (2008).

[30] P. Werner, T. Oka, and A. J. Millis, Phys. Rev. B **79**, 035320 (2009).

[31] D. Goldhaber-Gordon, H. Shtrikman, D. Mahalu, D. Abusch-Magder, U. Meirav, and M. A. Kastner, Nature (London) **391**, 156 (1998).

[32] S. M. Cronenwett, T. H. Oosterkamp, and L. P. Kouwenhoven, Science **281**, 540 (1998).

[33] W. G. van der Wiel, S. D. Franceschi, T. Fujisawa, J. M. Elzerman, S. Tarucha, and L. P. Kouwenhoven, Science **289**, 2105 (2000).